Applied Physics Letters

Mitigation of breathing oscillations and focusing of the plume in a segmented electrode wall-less Hall thruster

Cite as: Appl. Phys. Lett. **119**, 213501 (2021); https://doi.org/10.1063/5.0070307
Submitted: 05 September 2021 • Accepted: 07 November 2021 • Published Online: 22 November 2021

J. Simmonds and Y. Raitses

Applied Physics Letters ARTICLE scitation.org/journal/apl

Mitigation of breathing oscillations and focusing of the plume in a segmented electrode wall-less Hall thruster

Cite as: Appl. Phys. Lett. **119**, 213501 (2021); doi: 10.1063/5.0070307
Submitted: 5 September 2021 · Accepted: 7 November 2021 ·
Published Online: 22 November 2021

J. Simmonds[1,2,a] and Y. Raitses[1,a]

AFFILIATIONS

[1]Princeton Plasma Physics Laboratory, Princeton, New Jersey 08543, USA
[2]Department of Mechanical and Aerospace Engineering, Princeton University, Princeton, New Jersey 08543, USA

[a]Authors to whom correspondence should be addressed: jacobbs@princeton.edu and yraitses@pppl.gov

ABSTRACT

In the absence of the channel walls bounding the plasma, a wall-less Hall thruster is a promising configuration with a potentially longer lifetime and easier scalability than conventional Hall thrusters. Because the ion acceleration takes place in the fringing magnetic field with a strong axial component, the operation of a typical wall-less thruster is characterized by a large beam divergence of the plasma flow, which reduces the thrust. In this work, the addition of a biased segmented electrode to the wall-less thruster is shown to significantly narrow the plasma plume and suppress large amplitude breathing oscillations of the discharge current commonly associated with ionization instability. Both effects result in improvements to the thruster performance. Physical mechanisms responsible for these effects are unclear, but they are apparently associated with the reduction of the electron cross field transport to the anode and a transition in the breathing mode frequency.

Interest in deep-space missions has promoted research into long-lifetime plasma propulsion devices.[1–5] One approach to decrease Hall thruster erosion is the reduction or removal of the thruster channel walls facing the plasma. This approach was implemented and studied in a number of thruster concepts with crossed electric and magnetic fields, such as the wall-less and cylindrical Hall thrusters.[6–12] However, such designs tend to have larger plume angles and lower efficiencies than their conventional annular counterparts.[9,10,13] In the wall-less Hall thruster,[6–9] a fringing-kind magnetic field topology with a strong axial component of the magnetic field (Fig. 1) leads to the formation of radial electric fields, which accelerates ions out of the thruster radially. This causes plasma plume divergence and a reduction in thrust. In previous works, plume narrowing effects for annular and cylindrical Hall thrusters using segmented electrodes[13,29] and a plasma lens[14] have been demonstrated. In this work, we apply this approach to the wall-less Hall thruster,[9] which has a different E × B configuration, but still obtains similar narrowing of the plume. The result suggests this method to be a generalized approach to plume narrowing in such E × B plasma sources and thrusters. Moreover, we also report an unexpected effect of the segmented electrode on electron-cross field current and the breathing mode, leading to additional improvements of thruster performance. The breathing mode is a commonly reported plasma instability in Hall thrusters, which manifests as high-amplitude, low frequency (∼10 kHz) discharge current oscillations due to the periodic ionization of neutral propellant.[15]

The wall-less Hall thruster (Fig. 1) consists of a low-carbon steel magnetic circuit with a Samarium Cobalt (SmCo) permanent magnet, an anode which also serves as a gas-distributor, a dielectric backplate made from boron nitride ceramic to insulate the anode from the magnetic circuit, and a cathode neutralizer. The principle of operation of this thruster is expected to be generally similar to that of conventional Hall thrusters.[16] One of the key differences is in the enhanced role of the magnetic mirror at the center of the wall-less thruster, which forms a magneto-electrostatic trap (MET)[9] for electrons bouncing between the mirror and the plasma plume, which is at nearly the cathode potential. A key difference of the MET thruster utilized in this study from the other wall-less thrusters is the additional low magnetic-permeability stainless-steel electrode placed along the thruster edge, with magnetic field lines connecting the electrode and the center of the thruster (Fig. 1). This placement of the electrode was selected to implement a plasma lens effect[17] on the ions by increasing the plasma potential around the thruster edge to straighten outward-bound ions and lower plume divergence. This electrode is biased by a separate power supply with a variable voltage with respect to the cathode. Note

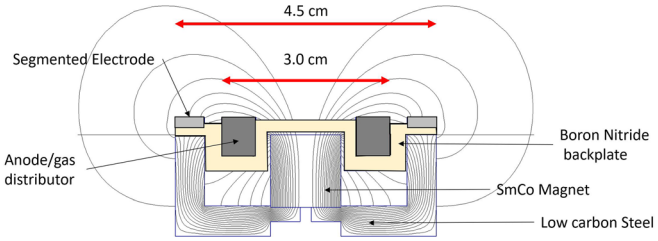

FIG. 1. Schematic and magnetic field lines of the segmented wall-less Hall thruster. Cathode-neutralizer is placed outside the thruster in the near plume and is not shown on this figure.

that segmented electrode here refers to an electrode segmented radially from the anode, whereas previous uses of the term segmented electrodes have referred to electrodes segmented axially[13] or azimuthally.[18]

The thruster was operated in the vacuum facility described elsewhere.[19] All experiments were conducted with xenon gas. The gas flow rate through the anode was 4, 6, and 8 sccm. A commercial hollow cathode was used as the cathode-neutralizer. The cathode flow rate was constant at 2 sccm. The discharge voltage between the thruster anode and the thruster cathode was 250 V. The bias voltage applied to the segmented electrode was varied. During the described experiments, the background gas pressure did not exceed 3×10^{-6} Torr. Finally, for diagnostics, we used a high resolution (± 0.1 mN) thrust stand and plume diagnostics, which are described elsewhere.[14,20]

Experiments demonstrated that the wall-less thruster exhibits a significant breathing mode of discharge current oscillations with amplitudes above 30% of the mean value. As the segmented electrode voltage increases from the floating value of +20 V with respect to the cathode, the amplitude of the breathing mode decreases to ~5%, particularly when the bias voltage is about 100 V (Fig. 2). Moreover, at the low flow rate of 4 sccm, a strong breathing mode caused unstable operation of the thruster. Stable operation at this flow rate was only possible with a voltage of at least 70 V applied to the segmented electrode.

This remarkable mitigation of the breathing mode was correlated with a decrease in the discharge current and an increase in current through the segmented electrode (Fig. 3). Interestingly, as the segmented electrode voltage increased above ~100 V, strong discharge current oscillations appeared again (Fig. 2). In these regimes, the thruster discharge becomes extremely unstable.

Curiously, the bias voltage of the segmented electrode has a profound effect on the frequency of the discharge current oscillations (Fig. 4). In principle, this effect seems to be similar to the effect of the anode voltage on the breathing mode frequency reported in Ref. 21. However, the effect of the anode voltage was not as strong as the effect of the segmented electrode reported in this paper. Indeed, as the bias voltage increases above ~80 V the oscillation frequency drops to about 60%–80% of the initial value for all regimes.

It appears that the discharges through the anode and the segmented electrode are coupled, as both the anode and outer current tend to oscillate with the same frequency in any given regime (Fig. 4). This coupling is likely due to the diffusion of electrons along and across magnetic field lines connecting the segmented electrode to that of the anode. Measurements from Figs. 3 and 4 suggest that the oscillation frequency is dependent upon which discharge dominates. At segmented electrode voltages below 70 V, the anode current exceeds that through the segmented electrode, the discharge frequency is relatively constant. However, as the outer current becomes comparable to the anode current, the discharge frequency drops abruptly and is also maintained at this lower value. This transition occurs at segmented electrode voltages corresponding to the suppression of the breathing mode of ~80 V (Fig. 2).

It is unclear why the frequency of the discharge current oscillations always drops to lower values and why the transition occurs so abruptly with the voltage bias of the segmented electrode. These low frequency oscillations are typically ascribed to an ionization instability (the breathing mode): An ionization front of high plasma density forms downstream and moves upstream toward the anode.[22,23] This ionization front grows as neutral propellant is ionized, depleting the local neutral density until the ionization rate diminishes due to low electron energy and the plasma dissipates. The low plasma density allows neutral propellant to fill the depleted region until another ionization front is formed in the high neutral density, allowing the process to repeat. The frequency of this repeatable process is then determined by the time at which the neutral atoms replenish the depleted region

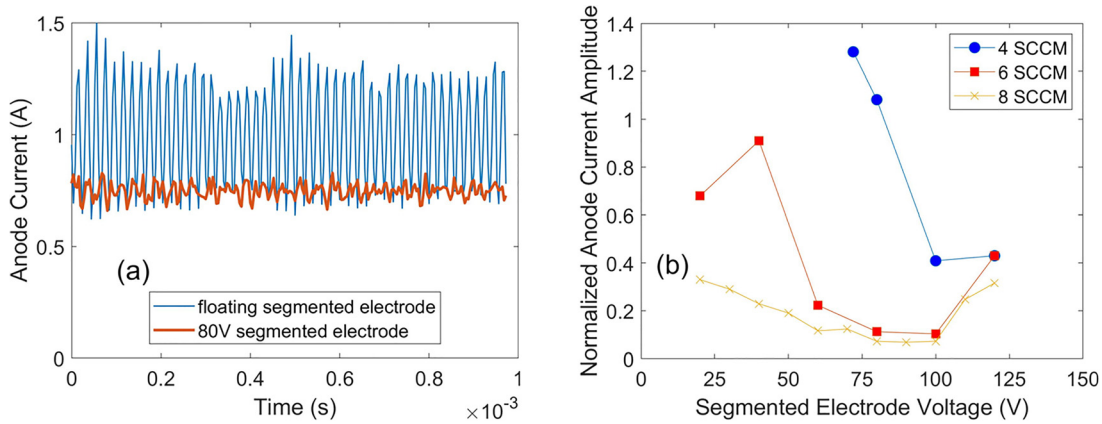

FIG. 2. Suppression of the breathing mode due to the bias of the segmented electrode shown by (a) anode current traces for 8 sccm mass flow and (b) normalized amplitudes over mass flows 4–8 sccm. Anode current amplitude is normalized by the time-average current, and the amplitude is derived from the RMS value.

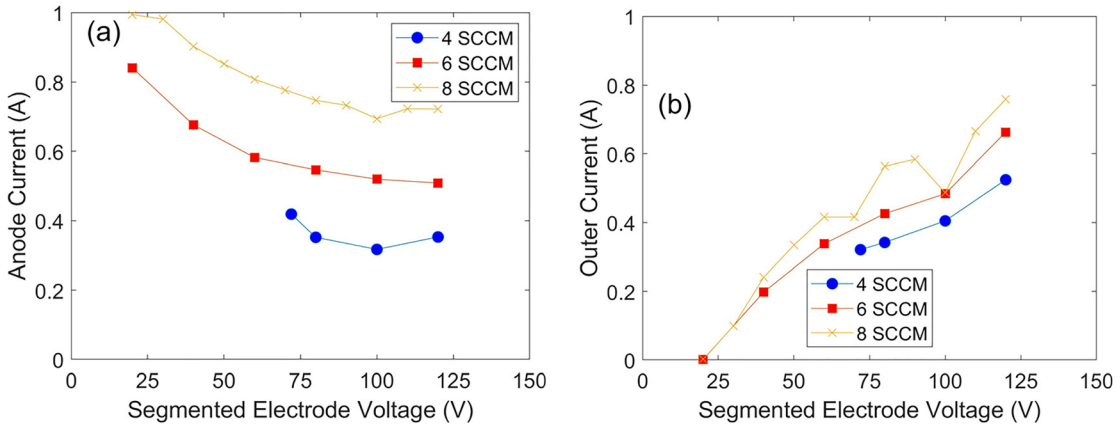

FIG. 3. Decrease in the anode current (a) and increase in the outer current through the segmented electrode (b) with the segmented electrode bias.

and the transient time of ions leaving the same region. Following this simplified description,[24,25] the breathing mode frequency ω can be estimated to be on the order of

$$\omega \sim \sqrt{\frac{u_i u_n}{L^2}}, \tag{1}$$

where u_i and u_n are the acoustic speeds of ions and neutrals and L is the ionization length. We assume the neutral speed to be constant as the segmented electrode voltage changes, and the ion velocity in this ionization region to be the Bohm velocity and to scale with $\sqrt{T_e}$, where T_e is the electron temperature. Previous works have shown a dependence upon the maximum electron temperature in a Hall thruster and the applied voltage.[26] If we assume the electron temperature scales with the discharge voltage of the dominating discharge, we expect a 60% decrease in oscillation frequency as the discharge transitions from the anode dominant regime ($250\ V$) to the segmented electrode dominant regime ($\sim 100\ V$) as the ions transit the ionization region more slowly.

Another plausible explanation for the effect of the segmented electrode on the frequency of breathing oscillations is associated with the backflow of ions from the ionization region to the anode/gas-distributor. It has been recently theorized that this backflow plays a critical role in determining the frequency of the breathing mode, as the neutral density near the anode is perturbed by wall recombination of the backflow ions causing the development of the ionization instability.[27] In principle, a similar process can also occur at the segmented electrode when the discharge between this electrode and the thruster cathode is accompanied by the ion backflow to this electrode. However, it is reasonable to expect that the ionization instability associated with this auxiliary discharge will require a longer time to develop because of lower plasma and neutral densities in this peripherical region of the MET thruster. As a result, both the ionization region and backflow region[25] are expected to be longer in length, which translates into a lower frequency of breathing oscillations of this discharge [see, for example, Eq. (1) and Ref. 27] as compared to the thruster discharge between the main anode and the cathode. Finally. we also note that measurements of nested Hall thrusters with multiple annular

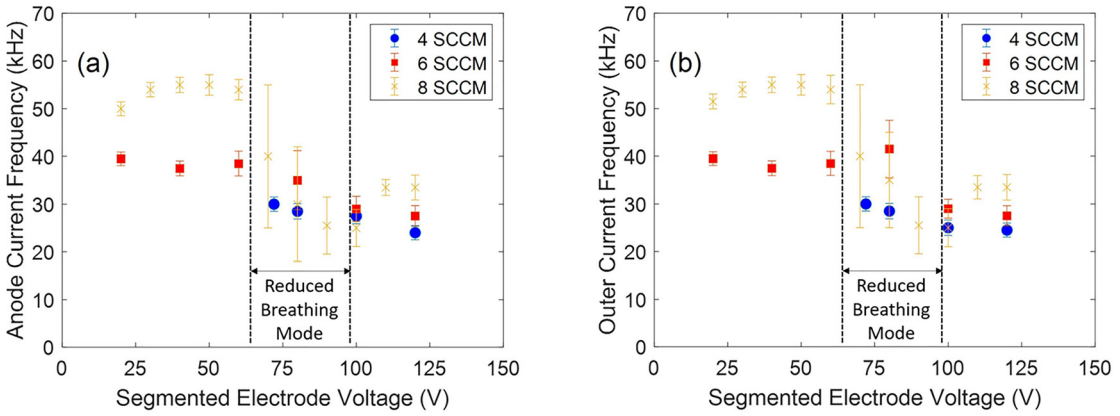

FIG. 4. Decrease in oscillation frequency as segmented electrode voltage increases for anode current (a) and outer current (b). Error bars correspond to the full-width-half-maximum of each fast Fourier transform frequency spectrum. Suppression regime for 6 and 8 sccm is highlighted between the dashed lines.

thruster channels, which have different magnitudes of the magnetic field (reducing toward the most outer channel) show a lower frequency of the breathing mode in the outer channel than that in the inner channel,[28] suggesting that other factors, such as lower magnetic fields, may come into play.

Regarding the abrupt suppression of the breathing oscillations observed at the certain bias voltages of the segmented electrode (~80 V), our hypothesis is that this is a result of the competition between the main thruster discharge and the segmented electrode discharge. Large amplitude oscillations of the discharge current (Fig. 2) occur when the feedstock of neutral atoms or plasma density is depleted over an oscillation. When the majority of the current is through one electrode, the frequency of the breathing oscillations is set by the geometry and plasma properties of the associated region [Eq. (1)] and the oscillations occur coherently. However, once the current is split between the two electrodes, there are two paths for the excess electrons generated by the breathing mode. The difference in the natural breathing mode frequencies in these discharges allows a persistent electron supply to be maintained, as electrons can diffuse between the outer electrode and anode region. This inhibits the buildup of the neutral density (and its perturbation due to wall recombination of the backflow ions) and prevents the growth of the ionization instability, which gives rise to large amplitude oscillations of the discharge current. The above phenomenological description can hint at an explanation toward why the frequency is constant with electrode voltage on either side of the voltage band corresponding to the suppression of the breathing mode. Two-dimensional or three-dimensional models are needed to fully understand this behavior, as the system with three electrodes (anode, segmented electrode, and the cathode) and two-dimensional magnetic field topology is quite complex.

It may be expected that providing an alternate electrode close to the cathode may increase the discharge power; however, it appears that total power decreases as the segmented electrode is applied, up to 50 W out of the nominal 210 W operation at 6 sccm (Fig. 5). These power reductions are considerable and appeared consistently. We note that the largest decrease in power occurred for the 6 sccm mass flow, which originally had a breathing mode current amplitude ~70% of the mean current. This power decreases as the current is diverted from the higher voltage anode to the lower voltage segmented electrode and increases again when this segmented electrode starts to dominate in current at high voltages.

Most surprising was the change in the thrust during this low-power regime. High current through the low voltage segmented electrode would imply that the ions are born in a low plasma potential and would accelerate with low energy. Thrust, however, increased up to 12% (Fig. 6). Measurements of the plasma plume in this regime showed some plume narrowing as the segmented electrode voltage was increased: at 8 sccm the 95% plume half-angle decreased from 57° nominal to 54° at 100 V segmented electrode bias. This corresponds to an expected $\frac{\cos 54^\circ}{\cos 57^\circ} = 8\%$ improvement in thrust. Over this range, the ion current in the plume remained relatively steady at 0.63 A with an associated propellant utilization of 110%, which is typical for this thruster due to multi-charged ions.[9] Similar plasma-focusing trends were observed at anode voltages of 350 V. The cause of this reduction in plume angle is also unclear. A plasma lens generated by the altered plasma potential profile may be focusing the ions as shown in other works.[14] Another potential mechanism is the reduction in central plasma pressure. Measurements have shown high plasma pressure in the middle of this wall-less Hall thruster[9] and by allowing electrons to flow along the magnetic field lines from the center to the outer segmented electrode this plasma pressure may be reduced, which would in turn reduce the associated radial electric fields.

In conclusion, the use of segmented electrodes appears to significantly alter the operation of the wall-less Hall thruster by focusing the ion trajectories, suppressing the discharge oscillations, and lowering the power draw of the device. The similar plume narrowing to the segmented annular Hall thruster[13] suggests that the careful placement of segmented electrodes may generally be advantageous for E × B plasma devices. Experiments revealed that the breathing mode oscillations appears to transition to a lower frequency as the segmented electrode bias increases, with suppression of the instability during this transition.

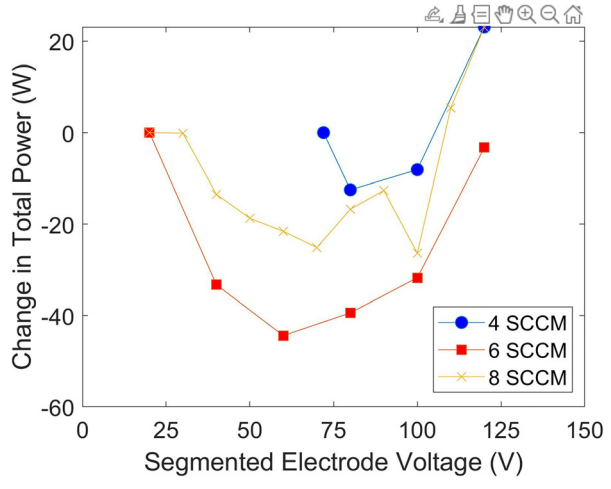

FIG. 5. Decrease in thruster power as the segmented electrode voltage increases from the nominal condition (4 sccm: 128 W, 6 sccm: 210 W, 8 sccm: 248 W). Thruster was unstable at 4 sccm without the biased segmented electrode, and so the 70 V bias was taken as the nominal power for this mass flow.

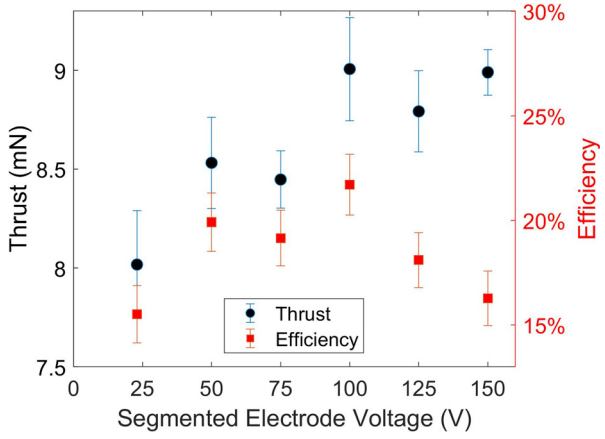

FIG. 6. Increase in thrust and efficiency as the segmented electrode voltage increases from the nominal condition of 250 V anode voltage and 8 sccm mass flow of Xenon.

This suppression is of practical importance to these devices, as it eliminates the need for filtering of the current through the power supply. The decrease in power and improvement in thrust resulted in a subsequent efficiency increase from 16% to 22%. While we have attempted to analyze the behavior of the ionization processes through discharge current traces of the two electrodes, more detailed plasma measurements and a self-consistent model would be beneficial to determine the validity of our suggested mechanisms of both the mitigation of the breathing oscillations and the plasma plume narrowing.

The authors would like to thank Professor Andrei Smolyakov for fruitful discussions and Tim Bennett and Peter Sloboda for technical assistance. This work is supported by the U.S. DOE under Contract No. DE-AC02-09CH11466.

AUTHOR DECLARATIONS

Conflict of Interest

Jacob Simmonds and Yevgeny Raitses have Provisional Patent 63/237,196 pending.

DATA AVAILABILITY

The data that support the findings of this study are available from the corresponding authors upon reasonable request.

REFERENCES

[1]J. Vaudolon, S. Mazouffre, C. Hénaux, D. Harribey, and A. Rossi, Appl. Phys. Lett. **107**, 174103 (2015).
[2]G. Teel, A. Shashurin, X. Fang, and M. Keidar, J. Appl. Phys. **121**, 023303 (2017).
[3]I. G. Mikellides, I. Katz, R. R. Hofer, and D. M. Goebel, Appl. Phys. Lett. **102**, 023509 (2013).
[4]Y. Ding, W. Peng, H. Sun, L. Wei, M. Zeng, F. Wang, and D. Yu, Jpn. J. Appl. Phys. **56**, 038001 (2017).
[5]V. H. Chaplin, R. B. Lobbia, A. Lopez Ortega, I. G. Mikellides, R. R. Hofer, J. E. Polk, and A. J. Friss, Appl. Phys. Lett. **116**, 234107 (2020).
[6]A. M. Kapulkin, A. D. Grishkevich, and V. F. Prisnyakov, in Proceedings of the 45th IAF Congress, Jerusalem, Israel, 9–14 October 1994 (1994).
[7]S. Mazouffre, S. Tsikata, and J. Vaudolon, J. Appl. Phys. **116**, 243302 (2014).
[8]B. Karadag, S. Cho, and I. Funaki, J. Appl. Phys. **123**, 153302 (2018).
[9]J. Simmonds and Y. Raitses, J. Appl. Phys. **130**, 093302 (2021).
[10]Y. Raitses, A. Smirnov, and N. J. Fisch, Appl. Phys. Lett. **90**, 221502 (2007).
[11]M. Seo, J. Lee, J. Seon, H. J. Lee, and W. Choe, Appl. Phys. Lett. **103**, 133501 (2013).
[12]H. Kim, W. Choe, Y. Lim, S. Lee, and S. Park, Appl. Phys. Lett. **110**, 114101 (2017).
[13]Y. Raitses, L. A. Dorf, A. A. Litvak, and N. J. Fisch, J. Appl. Phys. **88**, 1263 (2000).
[14]M. E. Griswold, Y. Raitses, and N. J. Fisch, Plasma Sources Sci. Technol. **23**, 044005 (2014).
[15]J.-P. Boeuf, J. Appl. Phys. **121**, 011101 (2017).
[16]A. I. Morozov and V. V. Savelyev, in *Reviews of Plasma Physics*, edited by B. B. Kadomtsev and V. D. Shafranov (Springer US, Boston, MA, 2000), pp. 203–391.
[17]A. I. Morozov, Dokl. Akad. Nauk SSSR **163**, 1363 (1965).
[18]Y. Shi, Y. Raitses, and A. Diallo, Plasma Sources Sci. Technol. **27**, 104006 (2018).
[19]Y. Raitses and N. J. Fisch, Phys. Plasmas **8**, 2579 (2001).
[20]Y. Raitses, E. Merino, and N. J. Fisch, J. Appl. Phys. **108**, 093307 (2010).
[21]T. Ito, N. Gascon, W. S. Crawford, and M. A. Cappelli, J. Propul. Power **23**, 1068 (2007).
[22]J. P. Boeuf and L. Garrigues, J. Appl. Phys. **84**, 3541 (1998).
[23]T. Lafleur, P. Chabert, and A. Bourdon, J. Appl. Phys. **130**, 053305 (2021).
[24]J. M. Fife, "Hybrid-PIC modeling and electrostatic probe survey of Hall thrusters," Doctoral dissertation (Department of Aeronautics and Astronautics, Massachusetts Institute of Technology, 1999).
[25]S. Barral and E. Ahedo, Phys. Rev. E **79**, 046401 (2009).
[26]Y. Raitses, A. Smirnov, D. Staack, and N. J. Fisch, Phys. Plasmas **13**, 014502 (2006).
[27]O. Chapurin, A. I. Smolyakov, G. Hagelaar, and Y. Raitses, J. Appl. Phys. **129**, 233307 (2021).
[28]M. S. McDonald, M. J. Sekerak, A. D. Gallimore, and R. R. Hofer, in *2013 IEEE Aerospace Conference* (IEEE, Big Sky, MT, 2013), pp. 1–12.
[29]N. Fisch, Y. Raitses, L. Dorf, and A. Litvak, J. Appl. Phys. **89**, 2040 (2001).